Characterization of free fatty acids photo-oxidation under UV radiations: A stepwise Raman study

Ali Assi, Rime Michael-jubeli, Arlette Baillet-guffroy, Ali Tfayli

A. Assi, R. Michael-Jubeli, A. Baillet-Guffroy, A. Tfayli, J Raman Spectrosc 2023, 54(1), 24.
https://doi.org/10.1002/jrs.6449

Characterization of free fatty acids photooxidation under UV radiations: a stepwise Raman study

Ali Assi, Rime Michael-Jubeli, Arlette Baillet-Guffroy, Ali Tfayli*

Author(s):

1- Ali Assi: ali.assi@universite-paris-saclay.fr , Lipides : systèmes analytiques et biologiques, Université Paris-Saclay, 91400, Orsay, France.

2- Rime Michael-Jubeli: rime.michael-jubeli@universite-paris-saclay.fr , Lipides : systèmes analytiques et biologiques, Université Paris-Saclay, 91400, Orsay, France.

3- Arlette Baillet-Guffroy: arlette.baillet-guffroy@universite-paris-saclay.fr , Lipides : systèmes analytiques et biologiques, Université Paris-Saclay, 91400, Orsay, France.

4- Ali Tfayli: **This author accept correspondance and proofs**, ali.tfayli@universite-paris-saclay.fr , Lipides : systèmes analytiques et biologiques, Université Paris-Saclay, 91400, Orsay, France.

To whom correspondence should be addressed : ali.tfayli@universite-paris-saclay.fr

Lip(Sys)², Chimie Analytique Pharmaceutique (FKA EA4041 Groupe de Chimie Analytique de Paris-Sud), Université Paris-Sud, Université Paris-Saclay, 91400, Orsay, France.

Abbreviations:

LPO: Lipid peroxidation.

MDA: Malondialdehyde.

PA: Palmitic acid.

SA: Stearic acid.

SB: Sebaleic acid.

OA: Oleic acid.

LA: Linolenic acid.

FWHM: Full width at half maximum.

Abstract

Lipid peroxidation (LPO) is an oxidative deterioration when oxidants such as reactive oxygen species attack lipids that contain double bonds especially polyunsaturated fatty acids (PUFAs). The mechanism of lipid peroxidation is composed of three steps: initiation, propagation and termination. It can result from several reaction pathways : (1) auto-oxidation, (2) enzymatic oxidation or (3) photo-oxidation.

UV solar exposition is a major concern in skin research, dermatology and cosmetic science. Skin surface lipids (SSLs) and *stratum corneum* (SC) lipids are among the first skin components exposed to external insults such as UV radiations. Fatty acids represent a major lipid class in SSLs and SC. The aim of this paper is to study the photo-oxidation of fatty acids under UV solar radiations using Raman spectroscopy. Vibrational spectroscopies are useful techniques to follow the LPO in its different stages of oxidation : (1) the initiation step by following the CH_2/CH_3 stretching bands ratio which decreases due to the hydrogen abstraction in alpha position, (2) the propagation step where primary oxidation products are formed such as hydroperoxides was evaluated by following the 1165/1640 cm^{-1} ((δ (OH) & v (C-O))/ v (C=O)) ratio which increases during oxidation process and finally the termination step that is marked by the formation of aldehydes, alcohols, ketone, *trans* secondary oxidation products and others were monitored by following the 1730/ 1640 cm^{-1} (v (C=O) (Ald.)/ v (C=O) (Acid)) ratio and the *trans* v (C=C)/*cis* v (C=C) ratio which increases indicating the formation of secondary oxidation products. To our knowledge, this work is the first to put together different spectral descriptors enabling to follow, step by step, the different modifications of free fatty acids structures during the oxidation process.

Keywords: Fatty acids, Lipid Peroxidation, Solar radiation, Vibrational spectroscopy, Malondialdehyde.

Introduction

Lipids are defined as biological substances that are generally hydrophobic non soluble in water and soluble in organic solvents such as chloroform [1,2].

Lipids are diverse hydrophobic or amphipathic organic compounds that act as structural components of cell membranes, sources of energy and important regulators of biological signaling pathways.

Characterization and separation of lipids by analytical and computational methods including liquid and gas chromatography coupled to Mass Spectrometry (MS) and nuclear magnetic resonance allowed the recognition of the essential role of lipids in the regulation of biological processes and in the progression of metabolic diseases including diabetes, obesity and even cancer [3].

Lipids are classified into eight groups: Fatty acyls, glycerolipids, glycerophospholipids, sphingolipids, sterol lipids, prenol lipids, glycolipids and polyketides. Each class is also divided into classes and sub classes. Fatty acyls in turn, contain not only fatty acids (FAs) but also numerous other functional groups such as alcohols, aldehydes, amines and esters [1].

Among all these classes and sub-classes, FAs are widely present in the human diet and are therefore predominant in human tissues. They consist of hydrocarbon chains of different lengths and degrees of unsaturations, with a carboxyl group at one end and a methyl group at the other [4]. FAs can be classified based on the number of double bonds in the acyl chain into saturated FAs, monounsaturated FAs and polyunsaturated FAs [5]. The number and orientation of these double bonds determine the biophysical properties

of FAs and overall structure [4,5]. FAs can also be divided into short, medium or long-chain FAs based on the number of carbon atoms [1].

In the skin, lipids are a principal constituent of the cutaneous skin barrier to prevent water loss, to protect skin from radiation and to prevent entry of harmful chemicals and organisms [6].

Free FAs constitute 10-20% of skin lipids (weight precent) which are mainly long-chain and saturated FAs localized in the epidermis [7]. FAs composition of the lipid bilayer influences membrane fluidity, interactions with membrane proteins, signal transduction pathways and defines cell type [4].

Lipid peroxidation (LPO) has been widely studied for several decades and has received an important attention in the field of medicine and biology, based on increasing evidence that LPO is implicated in the development of many chronic diseases such as cardiovascular disease, cancer, neurodegenerative diseases and aging [8,9].

In the skin, the generation of ROS (reactive oxygen species) from LPO oxidizes glycerophospholipids, sphingolipids, unsaturated fatty acids and cholesterol, which are the principal cutaneous lipid classes, inducing an alteration in barrier function and skin disorders including photoaging, skin cancer, atopic, dermatitis and psoriasis [7,10,11].

Therefore, the detection of modifications in lipid structure and analysis of lipid peroxidation products have garnered increased interest and have shown promising results in disease diagnosis where lipids can serve as potential biomarkers that not only aid in disease diagnosis but also provide prognostic insight into different diseases. This also highlights the importance of lipid-based studies in the design of targeted therapeutic strategies [12,13].

The first thing that pops into mind when talking about LPO is when oxidants such as free radicals attack lipids containing carbon-carbon double bond, especially polyunsaturated fatty acids (PUFAs) [14].

The general process of lipid peroxidation consists of three steps: initiation, propagation and termination. The initiation phase comprises hydrogen atom abstraction by free radicals (ROS) such as hydroxyl, alkoxyl and peroxyl producing a lipid radical, which in turn reacts with oxygen to produce hydroperoxides (LOOH) as primary products of LPO. Cleavage of LOOH results in formation of a variety of aldehyde products as secondary products such as malondialdehyde (MDA), 4-hydroxy-2-nonenal (HNE), 4-hydroxy-2-hexenal (4-HHE), acrolein and other minor products . The PUFAs with two or more double bonds are more prone to peroxidation [15,16].

Lipid peroxidation can result from several reaction pathways depending on the medium and the initiating agents: (1) auto-oxidation catalyzed by temperature, metal ions and free radicals, (2) enzymatic oxidation initiated by lipoxygenase or (3) photo-oxidation initiated by radiant energy such as UV, solar radiation or artificial light [8,9,17].

Solar radiation contains infrared (700-2500 nm), visible (400- 700 nm), and ultraviolet radiation (UVR) (290-400 nm). There are three types of UVR: UV-C rays (280-320 nm) filtered out by the ozone layer, UV-B (200-280 nm) and UV-A (320-400 nm). 95% of UV rays reaching the ground level are UV_A [18-20].

Solar UV radiations are known to have beneficial effects on the body such as stimulating the production of vitamin D [21].

However, ultraviolet (UV) radiation can induce oxidative stress that alters lipid composition. For example, studies show that UV radiation can affect FAs composition through dose-dependent increase in reactive oxygen species (ROS) and induction of lipid

peroxidation. In addition to promoting skin cancer through DNA damage, exposure to UV can alter the anti-cancer immune pathways which has been attributed to the change in lipid composition in the skin since lipids and lipid metabolism have been shown to directly affect immune cells phenotype. Acute UV exposure reduces free FAs and triglycerides in the epidermis which results in skin photoaging [22,23].

Oxidation of PUFAs is the main reaction responsible of the degradation of lipids [24]. The oxidative deterioration of polyunsaturated fatty acids generates a variety of aldehydic products including malondialdehyde (MDA) and 4-hydroxy-2-hexenal (4-HHE) who can be a relevant indicator of lipid peroxidation [25].

Many methods have been used to determine the degree of lipid peroxidation. The most used method for determination of MDA is the spectrophotometric detection of MDA at 532-535 nm after derivatization with thiobarbituric acid (TBA) but many studies have shown that interfering products are formed during the reaction of TBA with products of lipid peroxidation, inducing a decrease in the sensitivity of this method [26].

To avoid the problems of interference, a lot of HPLC methods have been described for measuring the MDA-TBA adduct or the MDA without derivatization [25-29].

Other authors described GC–MS methods using electron ionization (EI) for the measurement of MDA and other aldehydes [26].

Vibrational spectroscopy has also been used for the analyses of lipid peroxidation products [24,30-32]. It is well adapted for biological samples because it is a non-invasive method that requires little or no sample preparation and is rapid compared to time consuming chromatographic methods.

The generation of polar compounds (hydroperoxides) and carbonylic compounds (aldehydes) can be highly noticeable using FTIR while modifications upon the carbon

skeleton and C=C bonds of the FAs during oxidation and the appearance of *trans* double bonds are predicted to be seen in spectral changes using Raman spectroscopy [24,33].

The aim of this paper was to monitor and evaluate the modifications which may take place after solar irradiation on fatty acids using vibrational spectroscopy. Saturated and unsaturated FAs with different number of double bonds as well as different chain lengths were used.

Materials and methods

Chemicals

Linolenic Acid (LA), Oleic Acid (OA), Stearic Acid (SA), and Palmitic Acid (PA) were purchased from Sigma Aldrich (St Louis, MO, USA) and Sebaleic acid (SB) was purchased from Larodan (Solna, Sweden). Chloroform was purchased from Carlo Erba (Chaussée du Vexin, Val-de-Reuil, France). Lipid films are prepared by dissolving fatty acids in chloroform to obtain solutions of 2 mg/mL concentration. 20 µL of each solution was deposited on CaF_2 slides. The lipid films were then dried to remove residual solvent traces.

Samples irradiation

The four fatty acids were irradiated at different times using a solar simulator 16S-300 from a solar light company which produces a spectrum close to the solar spectrum. The power used for the irradiation was 0.52 W/cm^2. This power was measured using a pyranometer (Glenside, USA). Table 1 shows the different energies used during the irradiation process.

Time (min)	5	10	20	40	60	90	120	180	240
E J/cm²	156	312	624	1248	1872	2808	3744	5616	7488

Table 1: The different doses applied to fatty acids during irradiation in J/cm^2.

Raman spectroscopy

Raman spectral acquisitions were performed with an HR Labram microspectrometer (Horiba scientific, Palaiseau France). The excitation source is a 633-nm single-mode diode laser (TOPTICA PHOTONICS, Germany) with 35 mW laser power on the sample. The microspectrometer is equipped with an Olympus microscope, and measurements were recorded using a ×100 MPlan objective (Olympus, Japan). Light scattered by the sample is collected through the same objective. A Peltier cooled (−65 °C) multichannel coupled charge device (CCD) detector (1024×256 pixels) detects the Raman Stokes signal dispersed with a 400-μm slit width and a 600 grooves per millimeter holographic grating enabling a spectral resolution of 2 cm^{-1}. A calibration procedure was applied daily prior to data collection as recommended by Horiba Scientific. The zero-order position and the laser line were daily checked. Raman relative shift was checked on silica wafer band at 521 cm^{-1}. For the study, the selected spectral range was 400 - 3800 cm^{-1}. The acquisition of each spectrum required 3 min. Spectral acquisition was performed using Labspec6 software (Horiba Jobin Yvon SAS, Lille, France).

FTIR measurement

Spectral data was recorded using a Spotlight 400 infrared Spectrum (Perkin Elmer Life Sciences, Great Britain equipped with a liquid nitrogen cooled 16-pixel mercury cadmium telluride (MCT) line detector . Before each acquisition, a background is recorded on a clean part of the CaF_2 slide. All spectra were recorded in the mid infrared region (4000 to 750 cm^{-1}) at 30 scans/spectrum with a spectral resolution of 2 cm^{-1}.

9 different spectra were recorded for each slide. Data were pre-processed using Spectrum Image software.

Data analysis

IR and Raman data were analyzed with a software developed in house, that operates in the Matlab environment (The Matworks, Inc., Natick, MA, USA). The background, due to the fluorescence, was corrected using a polynomial function with a polynomial order of 4 [34]. All spectra were smoothed using Savitzky-Golay filter on 9 points with a polynomial order of 4 and normalized to the AUC of the CH stretching band. Automatic determination of the peak positions was performed using second derivatives.

Results and discussion:

Spectral characterization of fatty acids films before oxidation

Raman spectroscopy provides useful information to characterize the different fatty acids. Different spectral features can be used to monitor simultaneously the identity, the conformational behavior and the lateral packing of fatty acids.

At room temperature, Raman spectra of different fatty acids present differences due to the molecular structure, the conformational order, and the lateral packing (Fig. 1 and 2).

From a structural point of view, the presence of double bonds in the alkyl chains of fatty acids can be directly observed on the spectra. Unsaturated FAs selected to study in this work differ in the position and number of the double bonds that are reflected in their Raman spectra [5].

For these FAs, the band centered at about 1657 cm^{-1} is assigned to the v (C=C) stretching in *cis*-conformation while the bands arising at about 973 and 1267 cm^{-1} are associated with the C=C–H out-of-plane bending and the C=C–H in-plane bending respectively (Fig. 1.a, c and e). [5,35,36]

The v (C=O) stretching of the carboxylic acid presents a band at around 1640 cm^{-1} (1590-1645 cm^{-1}) that is overlapped by the strong v (C=C) stretching band. In infrared spectra, this band arises at around 1710 cm^{-1}. As shown in Figure 2, a shift of this band to the lower wavenumber and a peak splitting can be observed for saturated fatty acids, this is due to the polymorphism behavior of fatty acids [37].

On the other hand, for both infrared and Raman spectroscopy, the v (=CH) stretching modes can be identified by the vibration at about 3010 cm^{-1}. This band is attributed to the Vinyl CH stretch.

Finally, the presence of the double bonds in the hydrocarbon chains has a significant impact on both, the hydrocarbon chain conformational freedom and the nature of the H-bonds in the head group region and, consequently, on the lateral packing [38].

Lateral packing and conformational descriptors:

C–C stretching mode

In the fingerprint region, the bands between 990-1150 cm^{-1} are attributed to the C–C skeleton stretching mode and are very sensitive to their *trans–gauche* conformation order (the intramolecular interactions). The peaks at 1060 cm^{-1} and 1130 cm^{-1} correspond respectively to the asymmetric and symmetric v (C–C) in the *all-trans* chain segments. In addition, the band around 1100 cm^{-1} is also assigned to structures containing *trans* conformers. As for the *gauche* conformation, the bands in the skeletal optical region arise at about 1086 and 1113 cm^{-1} [5,35,36,38,39].

This region in the Raman spectra of saturated fatty acids SA and PA are characterized by sharp peaks and dominated by *trans* conformers (Fig. 1.b).

On the opposite side, this region for unsaturated fatty acids (OA, LA and SB) becomes a series of overlapping broad bands dominated by a central band at 1084 cm^{-1} as shown in Figure 1 indicating the presence of *gauche* conformation, that could be related to a higher mobility of the hydrocarbon skeleton with presence of unsaturation.

A problem identified in the literature is the inability to obtain absolute values for each conformation from the band intensities/positions and the fact that the changes are not linear [38].

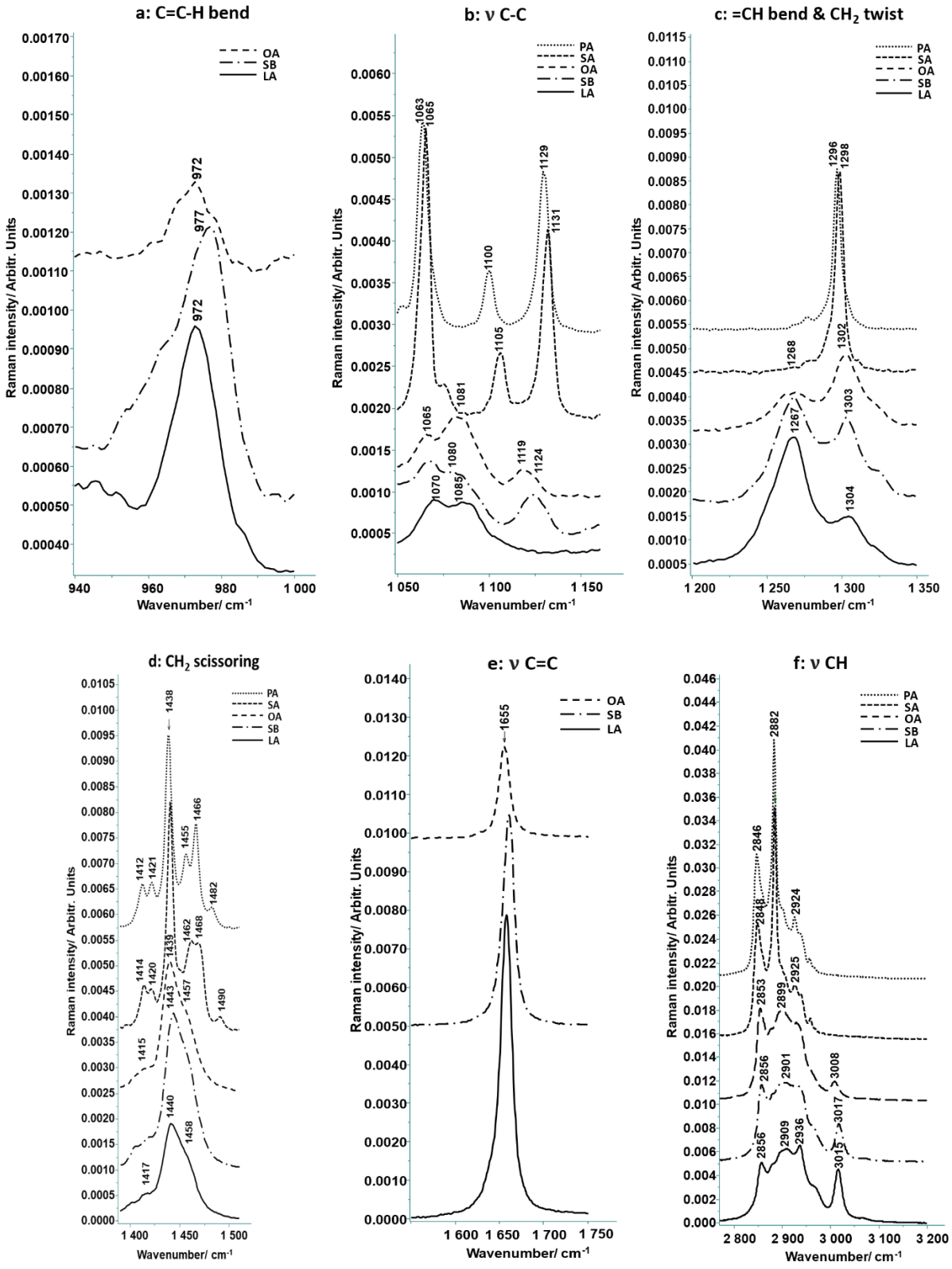

FIGURE 1 (A–F) Raman spectra of palmitic acid (PA), stearic acid (SA), oleic acid (OA), sebaleic acid (SB), and linolenic acid (LA) before UV irradiation. (A) C C H bend; (B) v C C; (C) CH bend and CH2 twist; (D) CH2 scissoring; (E) v C C; (F) v CH

CH_2 twisting

The Raman spectral feature at about 1300 cm^{-1} (Fig. 1.c) is assigned to the twisting of the CH_2 group. This band is sensitive to the conformational disorder; a sharp peak indicates an oriented hydrocarbon chain with high content of *trans* conformers. A shift to higher wavenumbers and a broadening of the band are indicative of an increase of the disorder and higher gauche conformers content [35,36].

As shown in Figure 1.c, low positions of the 1300 were obtained for saturated fatty acids (PA, SA) revealing a high interchain order, contrariwise a shift of this band to higher wavenumbers was observed for unsaturated FAs (OA, LA) indicating a significant increase of the interchain disorder and higher gauche conformers content.

Moreover, the FWHM was calculated for all Fatty acids to follow the broadening of the CH_2 twisting feature. OA, SB and LA present a FWHM of 19.34, 20.16 and 21.4 cm^{-1} respectively, almost three times the FWHM of PA (5.84 cm^{-1}) and SA (6.25 cm^{-1}). The values of FWHM confirm the information obtained from other spectral features on the conformational order/disorder, so with the increase of FWHM of CH_2 twisting the disorder increases.

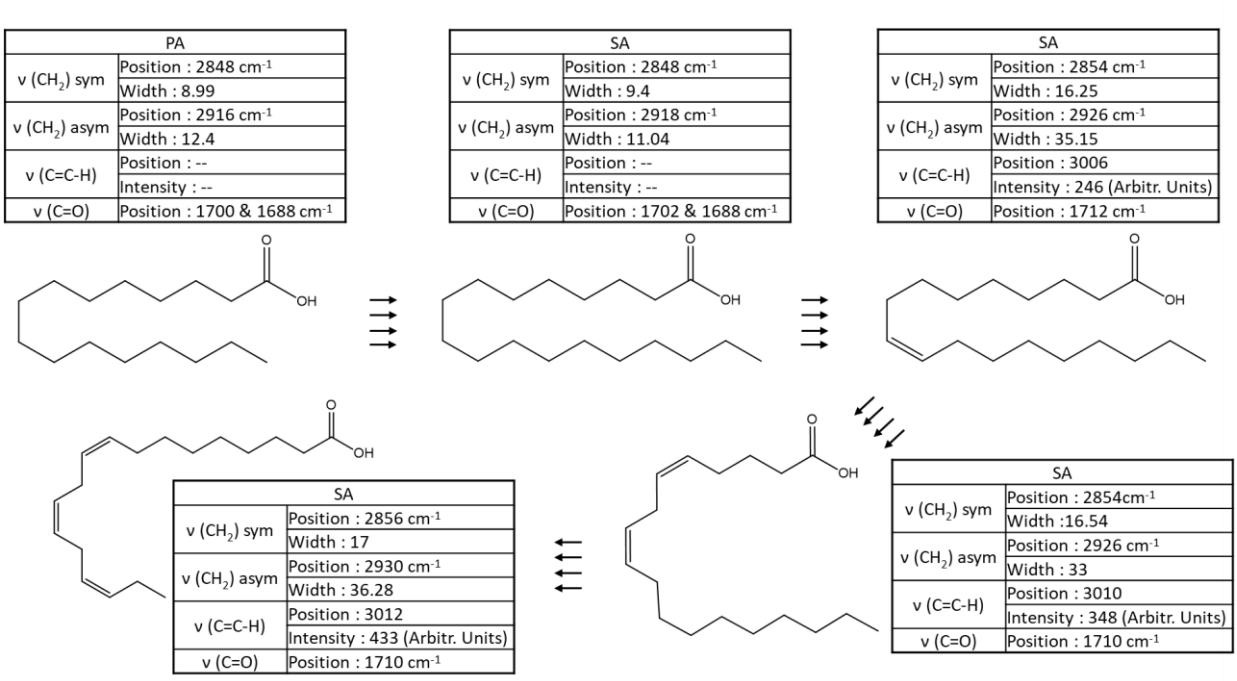

FIGURE 2 Infrared molecular descriptors of palmitic acid (PA), stearic acid (SA), oleic acid (OA), sebaleic acid (SB), and linolenic acid (LA) at room temperature

CH_2 Scissoring

Furthermore, the vibrational spectroscopies are used not only to observe the conformational order of the chain and the intramolecular behavior but also are useful for the determination of intermolecular chain packing arrangements [35,36].

The CH_2 scissoring band (1410 - 1485 cm^{-1}) is related to the lateral packing state (orthorhombic order, hexagonal order, and liquid-like chain packing). This spectral region is complex, with two to six apparently resolved observed bands. In fact, these bands are themselves not composed of pure CH_2 scissoring modes but contain contributions from vibrations of all the CH units present [35,36].

For unsaturated FA, the scissoring region shows one dominant band at around 1440 cm^{-1} with a strong shoulder at 1460 cm^{-1} (Fig. 1.d).

In contrast, for saturated FA the situation is more complex, with up to six main bands present in the CH_2 scissoring region of the spectrum. (Fig. 1.d) [38].

Additionally, in the presence of orthorhombic perpendicular sub-cell packing, the Raman spectra exhibit the factor group splitting of the CH_2 scissoring vibration band (1421 cm^{-1}), The splitting in this vibrational mode is due to the Fermi resonance with CH_2 rocking. This band is present for unsaturated FA and absent for saturated ones (Fig. 1.d). Moreover, a shift of the 1440 cm^{-1} band to higher wavenumbers is a manifestation of significant interchain disorder [35,36].

As illustrated in Figure 1.d, low positions of the 1440 were obtained for PA and SA revealing a high interchain order, contrariwise a shift of this band to higher wavenumbers was observed for unsaturated FAs (OA, SB, LA) indicating a significant interchain disorder.

Furthermore, the FWHM of the 1440 cm^{-1} was calculated. OA, SB and LA present a FWHM of 16.07, 18.65 and 20.49 cm^{-1}, respectively, which are greater than the FWHM of PA (7.46 cm^{-1}) and SA (8.25 cm^{-1}). These values of FWHM confirm the information obtained from the band position of 1440.

CH_2 and CH_3 stretching

The 2800-3000 cm^{-1} region is attributed to the stretching vibration of symmetric and asymmetric CH_2 and CH_3.

The bands at around 2850 cm^{-1} and 2880 cm^{-1} are associated with the symmetric and asymmetric CH_2 stretching, respectively in Raman spectra while in infrared, these bands occur at around 2850 and 2920 cm^{-1} respectively for CH_2 symmetric and asymmetric stretching.

The CH_3 symmetric and asymmetric stretching bands occur near 2934 and 2962 cm^{-1} respectively in Raman spectroscopy and at around 2870 and 2950 cm^{-1} in infrared spectroscopy [35,36,40-43].

As shown in Figure 1.f, the band at about 2850 cm^{-1}, that is assigned to the CH2 symmetric vibration, dominates for unsaturated FA (AL, AO) compared to the CH_2 asymmetric band, while for saturated FAs (PA, SA), the asymmetric vibration of CH_2 at about 2880 dominates [43].

Consequently, the broadening of the 2880 cm^{-1} band indicates motional freedom in the backbone which could be explained by the increase of the degree of unsaturation.

Afterwards, the structure of the CH-stretching region depends upon the interactions, enhanced by Fermi resonance, of CH-stretching fundamentals with CH deformation overtones [44].

Furthermore, this region is sensitive to the lateral packing of lipids, so taking the intensity ratio of ($\nu(CH_2)$ asym/$\nu(CH_2)$ sym) is an essential standard in vibrational spectroscopy studies performed on lipids because this peak ratio has been found to be sensitive to the hydrocarbon conformational order [35,36,45,46].

In other words, more gauche conformation of lipid alkyl backbone leads to an increase in the disordered lateral chain packing, whereas more *trans* conformation of lipids leads to an increase in the ordered lateral chain packing [39].

A high value of this ratio was obtained for saturated fatty acids (SA and PA) indicating a high conformational order of lipids.

This information is also confirmed by the position of the symmetrical CH_2 stretching. A low position is linked to a more ordered acyl chain.

In addition, information about organization can be obtained in infrared spectroscopy. The position and the bandwidth of the symmetric CH_2 stretching band are sensitive markers of the chain conformational order, a shift of this band to lower wavenumbers and an increase of the FWHM reveal a high ordered lateral chain packing. Also, the position and the intensity of the asymmetric CH_2 stretching could be a marker for conformational order thus with the decrease in order, the band shifts towards higher wavenumbers and decreases in intensity (Fig. 2).

The second part of the study in this paper is devoted to the behavior in the oxidation

1) Stearic, palmitic and Oleic acids:

SA and PA are saturated fatty acids with 18 and 16 carbons, respectively. OA is an unsaturated fatty acid with one unsaturation and 18 carbons.

When talking about lipid oxidation it is only the polyunsaturated fatty acids with 2 or more double bonds which are of interest. Saturated fatty acids are less vulnerable to lipid peroxidation than their unsaturated counterparts [47].

No modifications were observed in Raman and infrared spectra after an applied dose of 7488 J/cm^2 for the Palmitic and Stearic acids.

In addition, no significant variations of the *trans*/*gauche* ratio of the C-C stretching bond and of the $\nu(CH_2)$ asym/$\nu(CH_2)$ sym ratio were noticed for the palmitic and stearic acid during the irradiation (Data not shown).

As known, monounsaturated fatty acids are less prone to UV oxidation, but inexplicable modifications were observed at high doses for Oleic acid. For example, a marked increase

in the 1655-1675 cm^{-1}/2840-2890 cm^{-1} (**ν** (C=C)/ **ν** (CH)) ratio and a marked increase in 972 cm^{-1}/2840-2890 cm^{-1} (δ (=CH)/ **ν** (CH)) ratio were noticed at high doses. (Data not shown)

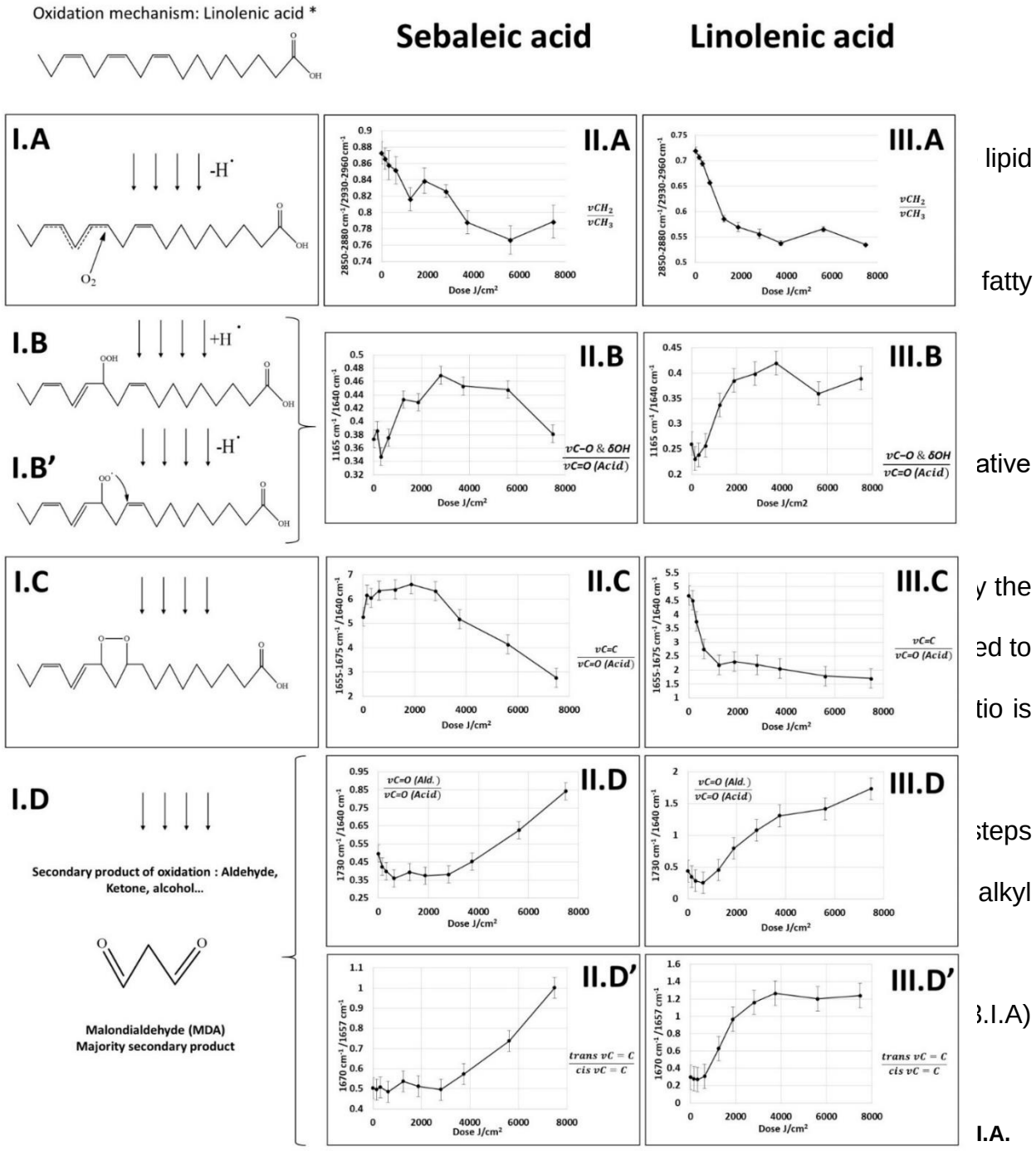

lipid

fatty

ative

y the

ed to

tio is

steps

alkyl

3.I.A)

I.A.

D.

formation of secondary oxidation products]. **II.** Raman descriptors of Sebaleic acid (SB) oxidation. **III.**

Raman descriptors of Linolenic acid (LA) descriptors. [**II, III.A.** CH_2/CH_3 stretching ratio. **II, III.B.** (δOH & vCO)/vC=O (acid) ratio. **II, III.C.** vC=C/vC=O (acid) ratio. **II, III.D.** vC=O (Aldehyde)/vC=O (acid) ratio. **II, III.D'.** *trans* vC=C)/*cis* vC=C ratio].

The formation of hydroperoxides can be monitored by following the relative evolution of the band at 1165 cm^{-1} that is assigned to the δ (OH) bending and ν (C-O) stretching.

For relative monitoring this band was divided by the 1640 cm^{-1} band associated to ν (C=O) stretching specific of carboxylic moieties. The choice of 1640 cm^{-1} band as internal standard is related to the fact that the carboxylic function remains intact during the oxidation process [24].

The 1165 cm^{-1}/1640 cm^{-1} ratio shows a significant increase after 624 and 156 J/cm^2 for SB and LA respectively indicating the beginning of hydro-peroxidation after these doses.

A plateau is then reached around 2808 J/cm^2 for SB and 1872 J/cm^2 for LA. This could be related to an equilibrium between hydro-peroxidation and the formation of peroxyl radicals by hydrogen abstraction (Fig. 3.I.B').

A decrease in the ratio's values is observed at 7488 J/cm^2 for SB and 5616 J/cm^2 for LA. This may be explained by higher peroxyl radicals formation. The variations in the 1165 cm^{-1} band are also observed directly on mean Raman spectra plotted in Fig. 4.A and 4.D.

The formation of hydroperoxides was also confirmed by the appearance of a broad band in the 3100-3600 cm^{-1} region that is assigned to the OH stretching in infrared spectra (Fig. 5).

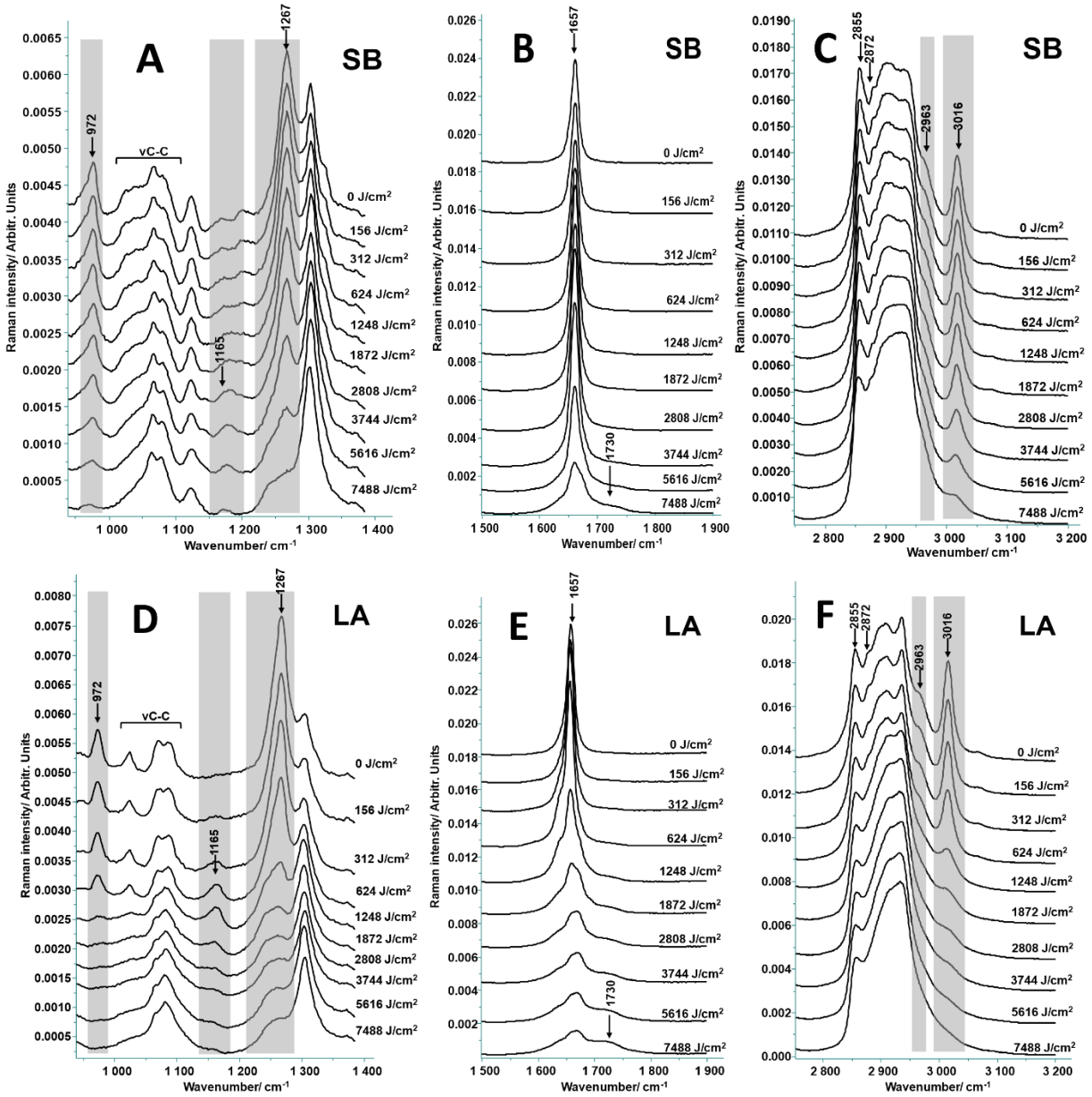

FIGURE 4 (A–F) Raman spectra of sebaleic acid (SB) and linolenic acid (LA) at different UV doses

Furthermore, the increase of this ratio and the appearance of the OH stretching band in infrared, are not only related to hydroperoxides but also to the formation of Alcohol as minority secondary oxidation products. This could explain the further increase of the 1165 cm^{-1}/1640 cm^{-1} ratio at 7488 J/cm^2 for LA. No similar observation can be seen for SB. This

can simply be connected to oxidation levels of both fatty acids at similar irradiation doses. LA with 3 doubles bonds is more prone to oxidation than SB with only 2 double bonds.

Hydroperoxides and peroxyl radicals are unstable and decompose to a variety of volatile compounds, including aldehydes, ketones, hydrocarbons, and other secondary products [54]. To lead to the formation of these secondary products, a cyclization mechanism is suggested (Fig. 3.I.C) to take place.

Cyclisation mechanism induces a loss of a double bond in the unsaturated fatty acid chain (Fig. 3.I.C). This can be followed by the relative evolution of the 1675 cm^{-1} (v (C=C)). Thus, the 1655-1675/1640 cm^{-1} (v (C=C) / v (C=O) Acid) was calculated and plotted in Fig. 3.II.C and 3.III.C.

For SB (Fig. 3.II.C), this ratio remains unchanged up to 2808 J/cm^2 dose of UV. After this dose, a marked decrease is observed in parallel with the up-described plateau in Fig. 3.II.B for the the δ (OH) bending and v (C-O) stretching relative evolution. This observation may confirm the balance between the different oxidation steps that may occur simultaneously.

In contrast, for LA (Fig. 3.III.C), the v (C=C) / v (C=O) ratio decreased directly after 156 J/cm^2. The abrupt decrease is simultaneous with the increase in the hydroperoxidation markers. This can be explained by instability of the LA. Different steps of the oxidation mechanism take place simultaneously for the different LA molecules present in the irradiated film. After 1248 J/cm^2 a plateau is observed with a slightly descending slope.

As described before, the final steps of the oxidation mechanisms lead to the formation of aldehydes, ketone, alcohols, and other secondary products. Malondialdehyde (MDA) was described as the major secondary product for polyunsaturated fatty acids (Fig. 3.I.D).

The formation of these products can be observed by the appearance of a shoulder at around 1730 cm^{-1} (Fig. 4.B and 4.E). This band can be attributed to the v (C=O) stretching of aldehyde. It's relative evolution (1730 cm^{-1}/1640 cm^{-1} (v (C=O) Ald./ v (C=O) Acid)) shows a marked increase after 2808 J/cm^2 for SB and 624 J/cm^2 for LA (Fig. 3.II.D and 3.III.D) [48,51,52]. This increase is observed up to 7488 J/cm^2 with a slight change in the slope after 3744 J/cm^2 for LA. Same observations were obtained from infrared measurements (data not shown).

In parallel, the increase in the *trans* v (C=C)/ *cis* v (C=C) ratio (Fig. 3.II.D' and 3.III.D') is also observed. The increase in the *trans* conformers was described by Muik et al. and was related to the formation of *trans* secondary oxidation products [24]. The conformers changes can also be seen by the broadening of the peak at around 1657 cm^{-1} in Raman spectra for both acids (Fig. 4.E and 4.A).

Furthermore, and as mentioned before, the fragmentation of the alkyl chain is confirmed by the decrease of the CH_2/CH_3 ratio after 2808 J/cm^2 and 1248 J/cm^2 for SB and LA, respectively (Fig. 3.II.B and 3.III.B).

In addition to the structural evolution, organizational and conformational changes are observed. Fig. 4.A and 4.D reveal an important broadening in the 1000-1125 cm^{-1} region

indicating a significant intrachain disorder and a high content of *gauche* conformers after UV irradiations.

Fig. 4.C and 4F show the decrease of the v (CH_2) asym shoulder at around 2870 cm^{-1} indicating higher interchain disorder along with irradiation. The decrease in the AUC of the 2870 cm^{-1} band may contribute in the observed decrease of the CH_2/CH_3 ratio.

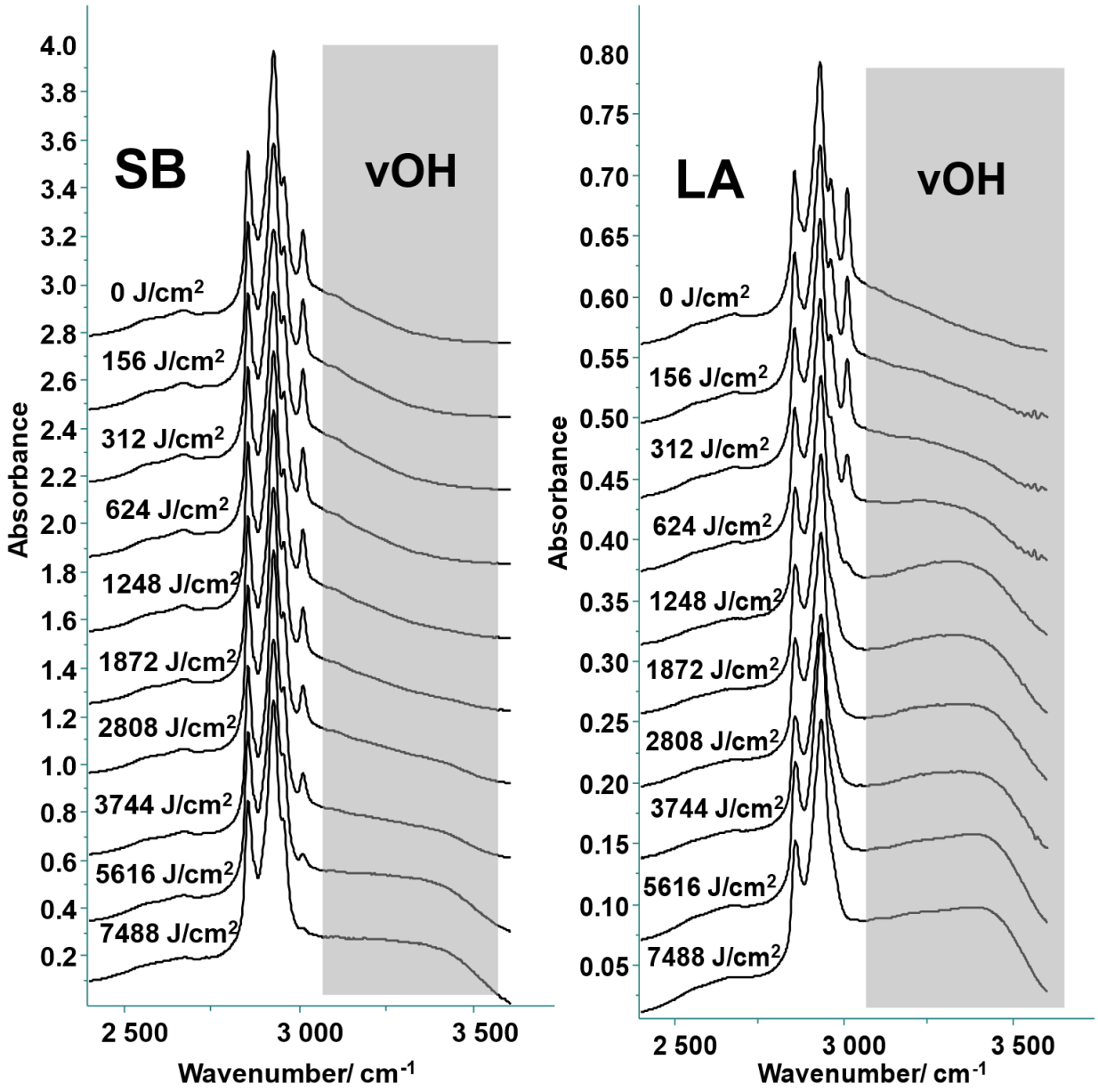

FIGURE 5 Infrared spectra (vCH region) of stearic acid (SA) and linolenic acid (LA) at different UV doses

Conclusion:

Skin Surface Lipids (SSLs) and stratum corneum (SC) lipids represent the first barrier protecting our body against external insults. Fatty acids are among the three major lipid classes within the SC along with ceramides and cholesterol. FAs also represent an important class in SSLs.

Solar UV exposition and photo-oxydation represent a major concern in skin research, dermatology, and cosmetic science. Even though the effect of UV radiations on epidermal and dermal components is extensively studied, their effect on lipidic barrier is generally observed from a functional point of view, *i.e.* the observation of the increase of transepidermal water loss (TEWL) *in vivo* [55-59]. *In vitro* studies on lipid films applied one or two given doses [60-63] and observations are made generally at the end of the oxidation process. In this paper, the use of Raman and Infrared spectroscopies enabled to monitor, step by step, the oxidation process of fatty acids induced by different doses of UV irradiations obtained under a solar simulator. Similar measurements will be performed on other lipid classes present in SSLs and SC.

To our knowledge, this work is the first to put together different spectral descriptors enabling to follow the different structural modifications during the oxidation process, *i.e.* hydrogen abstraction, formation of hydroperoxides and peroxyl radicals as primary oxidation products and the formation of aldehydes, ketones, alcohol as secondary products.

These formed products were followed by evaluating different Raman descriptors such as 1165/1640 cm^{-1} ratio to monitor the formation of hydroperoxides and alcohols, the CH_2/CH_3 stretching bands ratio for hydrogen abstraction and to follow the decomposition

of alkyl chains and the 1730/1640 cm^{-1} and *trans* v (C=C)/ *cis* v (C=C) ratio to evaluate the formation of aldehydes and other *trans* secondary oxidation products, respectively. The use of infrared spectroscopy confirmed the formation of hydroperoxides by a direct observation in the 3100-3600cm^{-1} region assigned to OH stretching and the secondary oxidation products such as aldehydes at ~1730 cm^{-1} associated to v (C=O) for aldehydes.

Compared to other techniques such as mass spectrometry, vibrational spectroscopy is a rapid, and non-destructive technique which would prove useful in future *in vivo* experiments that necessitate an unharmful method on living tissues and patients.

Acknowledgements

The authors would like to thank the Center of Research Pierre Fabre Dermo Cosmetics for the financial support of this work.

Conflict of interest: The authors declare that they have no conflict of interest.

References:

[1] Fahy E, Cotter D, Sud M, Subramaniam S *Biochimica et Biophysica Acta (BBA) - Molecular and Cell Biology of Lipids* **2011**, *1811*, 637.

[2] Prache N, *PhD thesis, Université Paris Saclay (COmUE), France*, 2017.

[3] Silva Barbosa Correia B, Torrinhas R, Ohashi W, Tasic L 2018, p https://www.intechopen.com/online.

[4] Burdge GC, Calder PC *World Review of Nutrition and Dietetics* **2014**, *112*, 1.

[5] Czamara K, Majzner K, Pacia MZ, Kochan K, Kaczor A, Baranska M *Journal of Raman Spectroscopy* **2015**, *46*, 4.

[6] Nicolaou A, Harwood J *Lipid Technology* **2016**, *28*, 36.

[7] Sjövall P, Skedung L, Gregoire S, Biganska O, Clément F, Luengo GS *Scientific Reports* **2018**, *8*, 16683.

[8] Shichiri M, Yoshida Y, Niki E In *Omega-3 Fatty Acids in Brain and Neurological Health*; Watson RR, De Meester F, Eds.; Academic Press: Boston, 2014, p 31.

[9] Spiteller G *Chemistry and Physics of Lipids* **1998**, *95*, 105.

[10] Lasch J, Schonfelder U, Walke M, Zellmer S, Beckert D *Biochim Biophys Acta* **1997**, *1349*, 171.

[11] Niki E *Free radical research* **2014**, *49*, 1.

[12] Stephenson DJ, Hoeferlin LA, Chalfant CE *Transl Res* **2017**, *189*, 13.

[13] Fuchs B, Bresler K, Schiller J *Chem Phys Lipids* **2011**, *164*, 782.

[14] Ayala A, Munoz MF, Arguelles S *Oxid Med Cell Longev* **2014**, *2014*, 360438.

[15] Catalá A, Díaz M *Frontiers in physiology* **2016**, *7*, 423.
[16] Spickett CM *Redox Biol* **2013**, *1*, 145.
[17] Sylvie E, *PhD thesis, Ecole polytechnique de l'Université de Nantes, France*, 2003.
[18] Johnson BE *Int J Cosmet Sci* **1983**, *5*, 131.
[19] Amaro-Ortiz A, Yan B, D'Orazio JA *Molecules* **2014**, *19*, 6202.
[20] Couteau C, Couteau O, Alami-El Boury S, Coiffard LJM *International Journal of Pharmaceutics* **2011**, *415*, 181.
[21] Berkey C, Oguchi N, Miyazawa K, Dauskardt R *Biochemistry and biophysics reports* **2019**, *19*, 100657.
[22] Tse BCY, Byrne SN *Photochem Photobiol Sci* **2020**, *19*, 870.
[23] Kim EJ, Jin XJ, Kim YK, Oh IK, Kim JE, Park CH, Chung JH *J Dermatol Sci* **2010**, *57*, 19.
[24] Muik B, Lendl B, Molina-Díaz A, Ayora-Cañada MJ *Chemistry and Physics of Lipids* **2005**, *134*, 173.
[25] Karatas F, Karatepe M, Baysar A *Anal Biochem* **2002**, *311*, 76.
[26] Zelzer S, Oberreither R, Bernecker C, Stelzer I, Truschnig-Wilders M, Fauler G *Free radical research* **2013**, *47*.
[27] Young IS, Trimble ER *Ann Clin Biochem* **1991**, *28 (Pt 5)*, 504.
[28] Dong X, Tang J, Chen X *Sci Rep* **2020**, *10*, 3990.
[29] Yonny ME, Rodríguez Torressi A, Nazareno MA, Cerutti S *Journal of Analytical Methods in Chemistry* **2017**, *2017*, 4327954.
[30] Machado NFL, de Carvalho LAEB, Otero JC, Marques MPM *Journal of Raman Spectroscopy* **2012**, *43*, 1991.
[31] Guillén MD, Cabo N *Journal of Agricultural and Food Chemistry* **1999**, *47*, 709.
[32] Agbenyega JK, Claybourn M, Ellis G *Spectrochimica Acta Part A: Molecular Spectroscopy* **1991**, *47*, 1375.
[33] Fan Y, Li S, Xu D-P *Guang pu xue yu guang pu fen xi = Guang pu* **2013**, *33*, 3240.
[34] Lieber CA, Mahadevan-Jansen A.
[35] Guillard E, Tfayli A, Manfait M, Baillet-Guffroy A *Anal Bioanal Chem* **2011**, *399*, 1201.
[36] Tfayli A, Guillard E, Manfait M, Baillet-Guffroy A *Anal Bioanal Chem* **2010**, *397*, 1281.
[37] L. da Silva LF, Andrade-Filho T, Freire PTC, Filho JM, da Silva Filho JG, Saraiva GD, Moreira SGC, de Sousa FF *The Journal of Physical Chemistry A* **2017**, *121*, 4830.
[38] Beattie JR, Bell SEJ, Moss BW *Lipids* **2004**, *39*, 407.
[39] Choe C, Lademann J, Darvin ME *Analyst* **2016**, *141*, 1981.
[40] Lin-Vien D, Ed.; Academic Press: Boston :, 1991.
[41] Yellin N, Levin IW *Biochimica et Biophysica Acta (BBA) - Lipids and Lipid Metabolism* **1977**, *489*, 177.
[42] Bulkin BJ, Krishnamachari N *Journal of the American Chemical Society* **1972**, *94*, 1109.
[43] Larsson K *Chemistry and Physics of Lipids* **1973**, *10*, 165.
[44] Verma SP, Wallach DFH *Biochimica et Biophysica Acta (BBA) - Lipids and Lipid Metabolism* **1977**, *486*, 217.

[45] Wegener M, Neubert R, Rettig W, Wartewig S *International Journal of Pharmaceutics* **1996**, *128*, 203.

[46] Snyder RG, Scherer JR, Gaber BP *Biochimica et Biophysica Acta (BBA) - Biomembranes* **1980**, *601*, 47.

[47] Rael L, Thomas G, Craun M, Curtis C *Journal of biochemistry and molecular biology* **2004**, *37*, 749.

[48] Frankel EN *Progress in Lipid Research* **1984**, *23*, 197.

[49] Shah D, Mahajan N, Sah S, Nath SK, Paudyal B *Journal of Biomedical Science* **2014**, *21*, 23.

[50] Niki E *Free Radic Biol Med* **2009**, *47*, 469.

[51] Girotti AW *Journal of Free Radicals in Biology & Medicine* **1985**, *1*, 87.

[52] Porter NA, Caldwell SE, Mills KA *Lipids* **1995**, *30*, 277.

[53] Michel F, Bonnefont-Rousselot D, Mas E, Drai J, Thérond P *Annales de Biologie Clinique* **2008**, *66*, 605.

[54] Cao J, Deng L, Zhu XM, Fan Y, Hu JN, Li J, Deng ZY *J Agric Food Chem* **2014**, *62*, 12545.

[55] Meguro S, Arai Y, Masukawa K, Uie K, Tokimitsu I *Photochem Photobiol* **1999**, *69*, 317.

[56] Gélis C, Mavon A, Delverdier M, Paillous N, Vicendo P *Photochemistry and Photobiology* **2002**, *75*, 598.

[57] Takagi Y, Nakagawa H, Kondo H, Takema Y, Imokawa G *J Invest Dermatol* **2004**, *123*, 1102.

[58] Yoon SH, Park JI, Lee JE, Myung CH, Hwang JS *Skin Pharmacol Physiol* **2019**, *32*, 254.

[59] Mac-Mary S, Sainthillier J-M, Jeudy A, Sladen C, Williams C, Bell M, Humbert P *Clinical interventions in aging* **2010**, *5*, 277.

[60] Trommer H *European Journal of Pharmaceutics and Biopharmaceutics* **2001**, *51*, 207.

[61] Trommer H, Bottcher R, Poppl A, Hoentsch J, Wartewig S, Neubert RH *Pharm Res* **2002**, *19*, 982.

[62] Merle C, Laugel C, Baillet-Guffroy A *Chem Phys Lipids* **2008**, *154*, 56.

[63] Merle C, Laugel C, Baillet-Guffroy A *Photochem Photobiol* **2010**, *86*, 553.

Time (min)	5	10	20	40	60	90	120	180	240
Total solar spectrum energy (J/cm²)	156	312	624	1248	1872	2808	3744	5616	7488
UV-B energy (J/cm^2)	0.45	0.9	1.8	3.6	5.4	8.1	10.8	16.2	21.6
Minimal erythemal dose	15 MED	30 MED	60 MED	120 MED	180 MED	270 MED	360 MED	540 MED	720 MED

Table 1: The different UV solar radiation doses applied to fatty acids during irradiation in J/cm^2.